

2-000051

44-168

ON THE FORMATION OF AURORAL ARCS

K. Stasiewicz

KGI PREPRINT 068

APRIL 1984



KIRUNA GEOPHYSICAL INSTITUTE  
KIRUNA SWEDEN

8

ON THE FORMATION OF AURORAL ARCS

by

Krzysztof Stasiewicz<sup>1)</sup>

Kiruna Geophysical Institute

P.O. Box 704, S-981 27 KIRUNA, Sweden

KGI Preprint 068

April 1984

1) on leave from:  
Polish Academy of Sciences  
Space Research Centre  
01-237 Warsaw, Poland

Printed in Sweden  
Kiruna Geophysical Institute  
Kiruna, 1984  
ISSN 0349-2656

ON THE FORMATION OF AURORAL ARCS

by

Krzysztof Stasiewicz\*

Kiruna Geophysical Institute

P. O. Box 704, S-981 27 KIRUNA, Sweden

Abstract

A new mechanism for auroral arc formation is presented. The characteristic linear shape of auroral arcs is determined by magnetically connected plasma clouds in the distant equatorial magnetosphere. These clouds originate as high speed plasma beams in the magnetotail and in the solar wind. It is found that the free energy for driving an auroral arc is provided by the difference of pressure between the cloud and the ambient plasma.

\* on leave from:

Polish Academy of Sciences

Space Research Centre

01-237 Warsaw, Poland

Auroral arcs are generally believed to be driven by an unidentified dynamo in the distant magnetosphere and/or the solar wind which forces electrons from the plasma sheet and/or the boundary layer to precipitate into the ionosphere. The earthward streaming electrons are subjected to an acceleration by field-aligned potential drops of 1-10 kV presumably at altitudes of about  $1 R_E$  before they generate an auroral display (for a review see refs 1-3). Despite considerable efforts which have been undertaken to study auroral phenomena some very fundamental questions still remain unanswered.

1. What determines the distinctive linear structure of discrete auroral arcs? ( $\sim 1 \times 1000$  km projected on a horizontal plane<sup>4-6</sup>);
2. What physical mechanism drives a field-aligned current system<sup>7,8</sup> associated with auroral arcs?

The height distribution of auroral luminosity can be explained<sup>9</sup> in terms of energy deposition by primary auroral electrons and is not discussed here. The first question was addressed many years ago by Störmer<sup>10</sup>; but his explanation based on the assumption of direct entry of solar particles is now known to be incorrect. It is also believed that auroral structures are the ionospheric footprints of some plasma objects in the magnetosphere which are projected earthward along the magnetic field lines. A median width of discrete auroral structures  $\approx 200$  m (lower limit  $< 70$  m and upper limit  $\approx 5000$  m)<sup>4</sup> corresponds to the gyroradius of a  $\approx 5$  keV proton in the ionosphere. Since 5 keV is a typical energy of plasma sheet protons we must look for a magnetospheric process which would result in the creation of thin plasma structures of the order of an ion gyroradius.

#### Why thin arcs?

An explanation for the thinness of magnetospheric plasma structures (and implicitly their footprints - auroral arcs) can be given on the basis of plasma behaviour derived from laboratory experiments. Specifically, it is known that plasma injected perpendicularly to a magnetic field of spatially in-

creasing strength can easily flow as a whole until it reaches a critical value  $B_c$  of the magnetic field strength which satisfies the pressure balance relation<sup>11,12</sup>

$$\frac{3}{2}\rho u_0^2 \approx E_c^2/2\mu_0 \quad (1)$$

where  $\rho = n(M+m)$  and  $u_0$  are the plasma density and the flow velocity, respectively. As the plasma flows across the magnetic field, a polarization electric field is set up allowing the beam to penetrate further due to the  $\underline{E} \times \underline{B}$  drift<sup>13,14</sup>. There is an obvious restriction that the potential difference across a plasma beam (width  $w$  perpendicularly to  $\underline{B}$ ) cannot exceed the voltage used to accelerate the beam which is equivalent to the kinetic energy of the beam ions  $eEw < Mu_0^2/2$ . Assume that the magnetic field is directed along the  $z$ -axis and  $u_0$  is directed along the  $x$ -axis. The polarisation electric field observed in the laboratory frame is  $E_y = u_0 B$  and we get an upper limit for the beam width

$$w < \frac{1}{2} g_i \quad (2)$$

where  $g_i = Mu_0/eB$  is the cyclotron radius of an ion with velocity  $u_0$  (not to be confused with a thermal cyclotron radius of the beam ions which is assumed to be much smaller). The relation (2) was first derived by Lindberg<sup>15</sup> in connection with his experiments with plasma beams. If the initial beam width is greater than (2) it either contracts<sup>15</sup> or splits up into field aligned flutes which satisfy (2). The latter behaviour was observed by Marković and Scott<sup>12</sup> and is schematically depicted in Fig 1.

An additional requirement<sup>16,17</sup> has to be satisfied in order to obtain the beam penetration due to the  $\underline{E} \times \underline{B}$  drift. The kinetic energy density of particles has to be sufficient to generate the electric field in the plasma volume

$$\frac{1}{2} nMu_0^2 \gg \frac{1}{2} E_y^2/\epsilon_0 \quad (3)$$

By using the relation  $E_y = u_0 B$  we can see that (3) is equivalent to

$$\omega_{pi}^2/\Omega_i^2 \gg 1 \quad (4)$$

where  $\omega_{pi}$  is the ion plasma frequency and  $\Omega_i$  is the ion gyrofrequency.

In the magnetotail  $\omega_{pi}^2/\Omega_i^2 \geq 10^5$ ; hence the above requirement is easily satisfied. High speed plasma flows ( $\sim 1000$ – $1500$  km/s) which considerably exceed the ion thermal velocity are indeed observed in the magnetotail<sup>18,19</sup>. Irrespectively of the actual physical process responsible for the acceleration, the earthward motion of such plasma streams in the equatorial plane should resemble the situation depicted in Fig.1. In fact such patterns are observed at the leading edge of westward traveling surges<sup>20</sup>. Observations of spatially narrow structures (or short-time bursts)<sup>21</sup> of high speed plasma flow in the plasma sheet are also in a qualitative agreement with this model. (An upper limit for the width of a beam  $u_0 \sim 1000$  km/s in the magnetic field  $B = 10$  nT is  $w \lesssim 500$  km).

The above considerations explain the emergence of thin plasma structures in the magnetosphere which due to their narrowness and unidirectional motion can be easily missed by a spacecraft not equipped with sophisticated particle instrumentation.

#### Why long arcs?

The horizontal extension of auroral arcs from a few hundred to a few thousand km indicates that plasma beams discussed in the previous section can cover large distances in the magnetosphere before they stop. In the laboratory situation the beam stops when the experiment configuration allows field-aligned currents to close outside the plasma and in this way neutralize polarisation charges in the plasma<sup>13</sup>. The time for establishing a current loop depends on the inductance of the whole circuit. In our case, this corresponds to the transit time of an Alfvén wave needed to transmit the electric field of the beam to the ionosphere, if the inertial effects of current carriers are neglected. By taking  $s \sim 15 R_E$  as the path length and  $v_A \sim 0.5 R_E/s$  as an average Alfvén velocity, we can estimate  $t_A \sim 30$  s as the minimum time for establishing the current loop between the beam and the ionosphere. If the leading edge of the plasma beam moves with  $u_0 \sim 1000$  km/s, the

beam can cover  $\approx 4 R_E$  before the current circuit is established. Thus, depolarization due to field-aligned currents can only stop the trailing part of the beam and in this way limit the beams length to a few Earth radii, if it was not limited earlier by the acceleration or injection process itself. Taking into account the convection velocity<sup>22</sup> of ambient plasma we can derive a better upper limit for the beam length

$$l_b < (u_o - u_c)s/v_A \quad (5)$$

where  $s$  is the path length measured along the field line,  $v_A$  is the average Alfvén velocity along this path and  $u_c$  is parallel to  $u_o$  component of the convection velocity.

The electric field reflected from the ionosphere is unable to affect the motion of the beam in the way discussed by Scholer<sup>23</sup> because the electric energy density is negligible in comparison to the kinetic energy density (cf. eqs. 3,4). A plasma cloud satisfying (5) will move decoupled from the ionosphere and we need to look for another mechanism to stop its motion. This can be constructed on the basis of the principle of conservation of energy. The kinetic energy of a particle, averaged over the gyration is  $W = Mu_o^2/2 + \mu B + Mv_{\parallel}^2/2$  where  $\mu = Mv_{\perp}^2/2B = W_{\perp}/B$  is the magnetic moment. The total particle energy of a plasma beam is

$$U_e = \int (\frac{1}{2} mu_o^2 + \mu_e B + W_{e\parallel} - e\Phi) ndV \quad (6a)$$

$$U_i = \int (\frac{1}{2} Mi_o^2 + \mu_i B + W_{i\parallel} + e\Phi) ndV \quad (6b)$$

$$U = U_e + U_i = \int (\frac{1}{2} nMu_o^2 + p_{\perp} + p_{\parallel}) dV \quad (6c)$$

where  $p_{\perp} = n(W_{e\perp} + W_{i\perp})$  and  $p_{\parallel} = n(W_{e\parallel} + W_{i\parallel})$  denote the perpendicular and the parallel pressure, respectively;  $\Phi$  is the potential of the large scale electric field in the magnetosphere and the integrals are over the beam volume.

Ambient magnetospheric particles which pass through the beam while they move along the field lines seem not to affect the energy balance. Although they acquire an electric drift velo-

city upon entering the beam they lose it while leaving the other side of the beam. The ambient particles which mirror just ahead of the beam either have to be pushed aside or will acquire the electric drift velocity. This will cause dissipation of the beam energy. For an estimation assume that ambient particles in the beam cross-section  $S$  acquire in average a fraction  $f < 1$  of the beam velocity. The change of the beam energy over the distance  $dx$  is  $d(\rho_b S l_b u^2/2) = -(\rho_a S f^2 u^2/2) dx$  where the subscripts  $b$  and  $a$  refer to the beam and to the ambient plasma, respectively. The solution of this equation is

$$u = u_0 \exp\left(-\frac{f^2 \rho_a x}{2 \rho_b l_b}\right). \quad (7)$$

When  $\rho_a = \rho_b$  and  $f=1$  the beam velocity is reduced by the factor  $e^{-1/2} = 0.6$  over the distance equal to its length  $l_b$ . This means that longer beams can move further.

Conservative fields can strongly affect the motion of a beam by increasing the thermal velocity of moving ions. The forward motion of the beam will cease when the ion thermal gyroradius becomes comparable to the beam width (2). This occurs in a region where  $v_{i\perp} \geq u/4$  or  $W_{i\perp} \geq Mu^2/32$ . From (6) we can see that the thermalization of ions is due to the conservation of the magnetic moment and due to magnetospheric electric fields (of the order of 2 kV/R<sub>E</sub> in the dawn-dusk direction)<sup>24</sup>. When the beam is directed toward the lower potential an increase of the ion parallel energy (leading to the increase of the ion gyroradius at mirror points) practically prevents any penetration because  $e\Delta\phi < Mu_0^2/32$ . The beam becomes a cloud with high parallel electron energy if it moves toward the higher potential. It can cover the longest distance if it moves straight along the equipotentials of the magnetospheric electric field<sup>24-26</sup>.

A combination of processes discussed in this section leads to the dissipation of the beam energy. When the beam is stopped it becomes an intruding plasma cloud with generally different parameters (e.g. electron pressure) than in the ambient mag-



netospheric plasma. If the beam moved close to the electric equipotentials, the resulting cloud can be projected along the magnetic field lines to a linear form resembling an auroral arc. Another question is now in order.

#### What drives an auroral display?

The boundary between the cloud and the ambient plasma is maintained in equilibrium by a magnetization current driven by the pressure gradient. A general expression for the perpendicular current in collisionless plasma is<sup>27</sup>

$$\underline{j}_\perp = \frac{B}{2} \times \left[ \underline{\nabla} p_\perp + (p_\parallel - p_\perp) \frac{\underline{\nabla} B}{B} + p \frac{d\underline{u}}{dt} \right] \frac{1}{(1-\alpha)} \quad (8)$$

where  $\alpha = \mu_0(p_\parallel - p_\perp)/B^2$  is an anisotropy parameter.

From the conservation of electric charges ( $\underline{\nabla} \cdot (\underline{j}_\perp + \underline{j}_\parallel) + \partial q/\partial t = 0$ ) we can derive an expression for field-aligned current. By noting that  $\underline{\nabla} \cdot \underline{j}_\parallel = B \partial (j_\parallel/B) / \partial s$  and calculating the divergence of  $\underline{j}_\perp$  given by (8) for an uniformly convecting plasma ( $d\underline{u}/dt=0$ ) we obtain<sup>28</sup>

$$B \partial [(1-\alpha) j_\parallel / B] / \partial s + (1-\alpha) \partial q / \partial t = -(1-\alpha)^{-1} (\underline{B} \times \underline{\nabla} B) \cdot \underline{\nabla} (p_\parallel + p_\perp) / B^3. \quad (9)$$

Integrating this equation along the field line between the conjugate ionospheres 'S' and 'N' we get

$$\left[ j_\parallel / B \right]_{s_S}^{s_N} + \frac{\partial}{\partial t} \int_{s_S}^{s_N} (1-\alpha) \frac{q}{B} ds = - \int_{s_S}^{s_N} \frac{\underline{\nabla} (p_\perp + p_\parallel) \cdot (\underline{B} \times \underline{\nabla} B)}{(1-\alpha) B^4} ds \quad (10)$$

$$= -2h \left\langle \frac{\underline{\nabla} p \cdot (\underline{B} \times \underline{\nabla} B)}{(1-\alpha) B^4} \right\rangle_c$$

where  $h$  is the extension ("height") of the cloud along the magnetic field,  $p = (p_\perp + p_\parallel)/2$ , and  $\langle \dots \rangle_c$  denotes an average over the integration interval (i.e. the height of the cloud). From (10) we can see that a field-aligned current and/or the charge separation occur whenever the pressure gradient has a component along the  $\underline{\nabla} B$  drift<sup>28,29</sup>. Such a configuration exists

at the boundary between an intruding cloud and the ambient plasma and results in the generation of a pair of oppositely directed field-aligned currents. The direction of parallel currents depends on the direction of the pressure gradient. Fig. 2 shows a current pattern implied by (10) when  $\nabla(p_{\perp} + p_{\parallel})$  is directed outward of a low pressure cloud. A high pressure cloud would generate a current pattern with opposite directions. Measurements of field-aligned currents<sup>7,8</sup> associated with premidnight auroral arcs give the same directions as the low-pressure cloud (Fig. 2). Rocket measurements<sup>30</sup> performed with a high spectral resolution over evening auroral arcs as well as satellite observations<sup>31</sup> indicate the presence of a two-temperature population of particles of magnetospheric origin (above the peak energy on the energy spectrum). Low-temperature magnetosheath-like electrons are superposed on a hotter population of plasma sheet electrons. A picture of plasma beams transporting earthward a cool boundary layer plasma from an acceleration region in the magnetotail is consistent with the above cited measurements.

For an estimation of the parallel current given by (10) assume  $\partial q/\partial t=0$ ,  $\alpha=0$ ,  $\nabla \cdot \underline{j}_{\perp} = 0$  outside the cloud and the symmetry of currents into the conjugate ionospheres. Denote by  $p_c$  and  $p_a$  the pressure  $(p_{\perp} + p_{\parallel})/2$  in the centre of the cloud and in the ambient plasma, respectively. The pressure gradient in (10) can be approximated by  $|\nabla p| = (p_a - p_c)/d$  and the dipole value of  $|\underline{B} \times \nabla B|/B^2$  is  $3/R_E L$  where  $d$  is the spatial scale for the pressure drop and  $L$  is the geocentric distance to the cloud in the Earth radii. The field-aligned current just above perpendicular currents flowing in the ionosphere is

$$j_{\parallel} = 10^{-5} (1-r) \frac{\beta h}{Ld} \quad (\text{A/m}^2) \quad (11)$$

where  $\beta = 2p_a \mu_0 / B^2$ ,  $r = p_c / p_a$  and the numerical factor is  $3B_I / 2R_E \mu_0$  ( $B_I = 5 \times 10^{-5} \text{T}$  denotes the magnetic field in the ionosphere). For  $L = 10$  we get  $j_{\parallel} > 1 \mu\text{A/m}^2$  when  $h > d / (1-r)\beta$ . The pressure drop occurs over the distance which cannot be larger than the half width of a cloud  $d < g_i / 4$ .

A low-pressure cloud  $p_C/p_a=0.5$  with a height of  $20g_i$  ( $\approx 1 R_E$ ) immersed in an ambient plasma of  $\beta \approx 1$  would generate  $j_{\parallel} \approx 40 \mu A/m^2$ . It is obvious that this mechanism can well explain even the strongest currents observed in association with auroral arcs. Note also the agreement of (11) with a generally observed anticorrelation between the current intensity  $j_{\parallel}$ <sup>8</sup> (or the optical luminosity<sup>5</sup>) and the width  $d$  of the current sheet.

The magnetospheric plasma has a limited ability to carry field-aligned currents. Only particles within a small loss cone  $<3^\circ$  can reach the ionosphere, severely limiting the magnetospheric electron current<sup>32-35</sup> (the ion current is negligible). On the other hand currents due to ionospheric particles are limited by current-driven instabilities<sup>36-39</sup>. For stronger currents or after the loss cone is depleted the charge accumulation (10) at the edges of a plasma cloud results in a buildup of parallel and perpendicular electric fields until the current determined by the RHS of (10) can flow along the field lines. A parallel voltage of 1-10 kV has to be established<sup>32-35</sup> in order to transmit the upward current greater than the loss-cone electron precipitation (typically  $<1 \mu A/m^2$ ). Given the long distance between the cloud and the ionosphere it is unlikely that simply the charge accumulation in certain flux tubes would create a kilovolt voltage in a process similar to charging a capacitor  $V(t)=Q(t)/C$ . Indeed, when the increasing electric field  $E_{\parallel}$  locally exceeds the Dreicer<sup>40, 41</sup> value ( $E_D=10^{-9} V/m$  for  $n \approx 30 \text{ cm}^{-3}$  and  $T_e=3 \text{ eV}$  at altitudes  $\approx 1 R_E$ )<sup>42</sup>, the runaway of thermal electrons is induced. This inevitably leads to the establishment of a turbulent region<sup>43, 44</sup> with anomalous resistivity<sup>36-39</sup> and/or distributed double layers<sup>45-49</sup>. The former mechanism is consistent with observed characteristics of the inverted-V electron spectra<sup>50</sup>. Magnetospheric electrons accelerated by parallel electric fields<sup>51, 52</sup> generated between the cloud and the ionosphere produce an auroral display (arc) as depicted in Fig. 2. The width of an arc is determined by the spatial scale of the pressure gradient which is expected to range from a few

electron gyroradius up to the half width of a cloud. Note that only electron parameters are likely to vary across the cloud. A large ion gyroradius would probably smear out any difference in ion parameters.

The total free energy available for the whole auroral process is  $\approx |p_a V - \int p dV| \approx \epsilon V$  where the integration is over the cloud volume and  $\epsilon = |p_a - p_c|$  is an average free energy density. Dividing the energy volume by its outflux rate we can estimate the duration of an auroral display

$$t_a \approx \frac{\epsilon h}{2k J_e} \left( \frac{B_I}{B_M} \right) \quad (12)$$

where  $J_e$  is the total energy flux into the ionosphere;  $k < 0.5$  denotes the fraction of the cloud surface ( $\perp B$ ) generating the upward current; and  $B_I/B_M$  is for the ratio of a magnetic flux tube surface at the magnetospheric cloud and at the ionosphere. A typical value of the energy flux due to precipitating auroral particles is<sup>53</sup>  $J_e \approx 10 \text{ erg} \cdot \text{cm}^{-2} \cdot \text{s}^{-1}$ . Multiplying this value by 2 (in order to account roughly for the ionospheric  $\underline{j} \cdot \underline{E}$  dissipation), and assuming:  $\epsilon = 1 \text{ keV} \cdot \text{cm}^{-3}$  ( $\approx 1.6 \times 10^{-9} \text{ erg} \cdot \text{cm}^{-3}$ ),  $h = 1 R_E$ ,  $k = 0.5$ , and  $B_I/B_M = 1000$ ; we obtain from (12)  $t_a \approx 50 \text{ s}$ . This value compares well with the observed duration of auroral arcs ( $\sim 10$ - $1000 \text{ s}$ ).

#### Summary and conclusions

The main points of the proposed model are:

1. An auroral arc corresponds to the upward current sheet generated at the magnetically connected edge of a distant plasma cloud. Such clouds originate in the magnetotail as high speed ( $u_0 \gg v_{ti}$ ) plasma beams.
2. The perpendicular to  $\underline{B}$  motion of a beam is due to the polarization electric field ( $\underline{E} \times \underline{B}$  drift) when the width and the length of the beam is constrained by eqs (2) and (5), respectively.

3. After the beam is stopped it becomes an intruding plasma cloud with different pressure than in the ambient plasma. A pressure gradient at the boundary between the cloud and the ambient plasma drives a magnetization current that leads to the electric charge separation and to a pair of field-aligned currents.
4. Field-aligned currents carried by hot magnetospheric particles are limited by a small loss-cone while currents due to ionospheric particles are constrained by current driven instabilities. When these limits are exceeded a charge accumulation at the edges of the plasma cloud generates perpendicular and induces parallel electric fields between the cloud and the ionosphere. Magnetospheric electrons accelerated earthward by parallel electric fields produce an auroral display in the ionosphere.

The above outline seems to provide a plausible basis for construction of a unified theory of structured auroral displays. The observed deformations, curls and motion<sup>54, 55</sup> of auroral structures presumably could be explained by taking into account inhomogeneities within plasma clouds and by considering the electromagnetic forces which act on them. A detailed analysis of eq. (10) is expected to reveal the time variation in currents and space charges what could account for the observed variations in auroral luminosity. Thicker auroral structures can be attributed to larger clouds which are transported from the tail by convection electric field so they do not need to satisfy (2). They can also result from plasma beams moving across the electric equipotentials. Note that eqs. (8-12) can be applied to plasma structures of arbitrary size.

Auroral arcs can be divided topologically into 3 groups: night side, day side (both groups roughly along the auroral oval) and polar cap arcs<sup>6, 56, 57</sup>. The day-side arcs form a fan-like structure on both sides of the noon meridian and are located equatorward of the cusp and do not connect with the night-side arcs. Although the illustration presented in this paper

(Fig. 2) applies only to arcs in the night-side auroral oval - the proposed model is capable of explaining other kinds of arcs as well. A particular implication of this model is that the day-side auroral arcs are the ionospheric footprints of solar wind plasma beams penetrating through the magnetopause and the low-latitude boundary layer<sup>58-60</sup>. Note that the relation (2) limits the width of penetrating structures to  $w < 100$  km when  $u_0 < 500$  km/s and  $B > 20$  nT, but dimensions of the resulting clouds are not limited. Polar cap arcs could correspond to solar wind elements penetrating through the plasma mantle<sup>61</sup> into the magnetospheric lobes and to magnetotail beams propagating perpendicularly to the equatorial plane.

#### Acknowledgements

The author would like to thank B. Hultqvist, R. Lundin and A. Steen for their inspiration to this work. I am indebted to B. Hultqvist for valuable discussions which resulted in a significant improvement of the original manuscript, and to M. Baron of EISCAT for reading the manuscript and helpful comments.

## Figure captions

Figure 1 A schematic picture of a plasma beam penetration into perpendicular magnetic field. The width of  $\underline{E} \times \underline{B}$  penetrating structures is constrained by the half of an ion gyroradius  $w < r_u/2eB$ .

Figure 2 Establishment of field-aligned currents driving an auroral arc due to the presence of a low-pressure plasma cloud in the equatorial magnetosphere. Symmetrical currents into the conjugate ionosphere are not shown.

## References

1. Akasofu, S.-I. & Kan, J.k., eds. Physics of Auroral Arc Formation (AGU, Washington, D.C., 1981)
2. Hultqvist, B. & Hagfors, T., eds. High-Latitude Space Plasma Physics (Plenum Press, New York, 1983)
3. Russell, C.T., ed. Auroral Processes (Japan Scientific Societies Press, Tokyo, 1979)
4. Maggs, J.E. & Davis, T.N., Planet. Space Sci. 16, 205-209 (1968)
5. Davis, T.N., Space Sci. Rev. 22, 77-113 (1978)
6. Akasofu, S.-I. & Kan, J.R., Geophys. Res. Lett. 7, 753-756 (1980)
7. Cloutier, P.A., Anderson, H.R., Park, R.J., Vondrak, R.R., Speiger, R.J. & Sandel, B.R., J. Geophys. Res. 75, 2595-2600 (1970)
8. Anderson, H.R. & Vondrak, R.R., Rev. Geophys. Space Phys. 13, 243-262 (1975)
9. Banks, P.M., Chappell, C.R. & Nagy, A.F., J. Geophys. Res. 79, 1459-1470 (1974)
10. Störmer, C., The Polar Aurora (Clarendon Press, Oxford, 1955)
11. Tuck, J.L., Phys. Rev. Lett. 3, 313-315 (1959)
12. Marković, P.D. & Scott, F.R., Phys. Fluids 14, 1742-1747 (1971)
13. Baker, D.A. & Hammel, J.E., Phys. Rev. Lett. 8, 157-158 (1962); Phys. Fluids 8, 713-722 (1965)
14. Ishizuka, H. & Robertson, S., Phys. Fluids 25, 2353-2358 (1982)
15. Lindberg, L., Astrophys. Space Sci. 55, 203-225 (1978)
16. Schmidt, G., Phys. Fluids 3, 961-965 (1960)
17. Peter, W. & Rostoker, N., Phys. Fluids 25, 730-735 (1982)
18. Frank, L.A. & Ackerson, K.L., J. Geophys. Res. 81, 5859-5881 (1976)
19. Hones, E.W., Bame, S.J. & Asbridge, J.R., J. Geophys. Res. 81, 227-234 (1976)
20. Kamide, Y. & Rostoker, G., J. Geophys. Res. 82, 5589-5608 (1977)



21. Coroniti, F.V., Frank, L.A., Williams, D.J., Lepping, R.P., Scarf, F.L., Krimigis, S.M. & Gloeckler, G., J. Geophys. Res. 85, 2957-2977 (1980)
22. Axford, W.I. Rev. Geophys. 7, 421-459 (1969)
23. Scholer, M., Planet. Space Sci. 18, 977-1004 (1969)
24. Kivelson, M.G., Rev. Geophys. Space Phys. 14, 189-197 (1976)
25. Volland, H., Ann. Geophys. 31, 154-174 (1975)
26. Stern, D.P., Rev. Geophys. Space Phys. 17, 626-640 (1979)
27. Parker, E.N., Phys. Rev. 107, 924-933 (1957)
28. Vasyliunas, V. M., in Particles and Fields in the Magnetosphere (ed. Mc Cormac, B. M.) 60-71 (D. Reidel, Holland, 1970)
29. Boström, R., in Physics of the hot plasma in the magnetosphere (eds. Hultqvist, B. & Stenflo, L.) 341-362 (Plenum, New York, 1975)
30. Sandahl, I., Eliasson, L. & Lundin, R., ESA SP-152, 257-262 (1980)
31. Burke, W. J., Silevitch, M. & Hardy, D. A. J. Geophys. Res. 88, 3127-3137 (1983)
32. Knight, S., Planet. Space Sci. 21, 741-750 (1973)
33. Lemaire, J. & Scherer, M., Planet. Space Sci. 22, 1485-1490 (1974)
34. Chiu, Y. T. & Schultz, M., J. Geophys. Res. 83, 629-642 (1978)
35. Lennartsson, W., Planet. Space Sci. 28, 135-147 (1980)
36. Kindel, J.M. & Kennel, C.F., J. Geophys. Res. 76, 3055-3078 (1971)
37. Papadopoulos, K., Rev. Geophys. Space Phys. 15, 113-127 (1977)
38. Galeev, A.A. & Sagdeev, R.S. in Review of Plasma Physics (ed. Leontovich, M. A.) v.7, 1-175 (Consultants Bureau, New York, 1979)
39. Dum, C. T. in Physics of Auroral Arc Formation (eds. Akasofu, S-I. & Kan, J. R.) 408-417 (AGU, Washington, D.C., 1981)
40. Dreicer, H., Phys. Rev. 115, 238-246 (1959)

41. Kalsrud, R.M., Sun, Y-C., Winsor, N.K., Fallon, H.A.,  
Phys. Rev. Lett. 31, 690-693 (1973)
42. Mozer, F.S., Cattell, C.A., Temerin, M., Torbert, S., Von  
Glinski, S., Waldorff, M. & Wygant, J., J. Geophys. Res.  
84, 5875-5884 (1979)
43. Gurnett, D.A. & Frank, L.A., J. Geophys. Res. 82,  
1031-1050 (1977)
44. Kintner, P.M., in High-Latitude Space Plasma Physics  
(eds. Hultqvist, B. & Hagfors, T.) 399-413 (Plenum Press,  
New York, 1983)
45. Shawhan, S.D., Fälthammar, C-G. & Block, L.P., J.  
Geophys. Res. 83, 1049-1054 (1978)
46. Torvén, S. in Wave Instabilities in Space Plasmas (eds.  
Palmadesso, P. J. & Papadopoulos, K.) 109-128 (D. Reidel,  
Holland, 1979)
47. Block, L., in Magnetospheric Currents (ed. Potemra, T.A.)  
315-324 (AGU, Washington, D.C., 1984)
48. Hudson, M. K., Lotko, W., Roth, I. & Witt, E. J. Geophys.  
Res. 88, 916-926 (1983)
49. Temerin, M., Cerny, K., Lotko, W. & Mozer, F.S. Phys. Rev.  
Lett. 48, 1175-1179 (1982)
50. Stasiewicz, K., Planet. Space Sci. 32, 379-389 (1984)
51. Mozer, F.S., Cattell, C.A., Hudson, M.K., Lysak, R.L.,  
Temerin, M. & Torbert, R.B., Space Sci. Rev. 27, 155-213  
(1980)
52. Fälthammar, C-G., ESA Journal 7, 385-404 (1983)
53. Lyons, L.R., Evans, D.S. & Lundin, R. J. Geophys. Res.  
457-461 (1979)
54. Hallinan, T.J. & Davis, T.N., Planet. Space Sci. 18,  
1735-1744 (1970)
55. Oguti, T., in Physics of Auroral Arc Formation (eds.  
Akasofu, S.-I. & Kan, J.R.) 31-41 (AGU, Washington, D.C.,  
1981)
56. Lassen, K. & Danielsen, C., J. Geophys. Res. 83, 5277-5284  
(1978)
57. Meng, C-I., Space Sci. Rev. 223-300 (1978)
58. Lemaire, J. & Roth, M., Planet. Space Sci. 29, 843-849  
(1981)

59. Paschmann, G., Scopke, N., Haerendel, G., Papamastoralis, J., Bame, S.J., Asbridge, J.R., Gosling, J.T., Hones, E.W. & Tech, E.R., Space Sci. Rev. 22, 717-737 (1978)
60. Eastman, T.E. & Hones, E.W., J. Geophys. Res. 84, 2019-2028 (1979)
61. Lundin, R. & Aparicio, B., Planet. Space Sci. 30, 81-91 (1982)

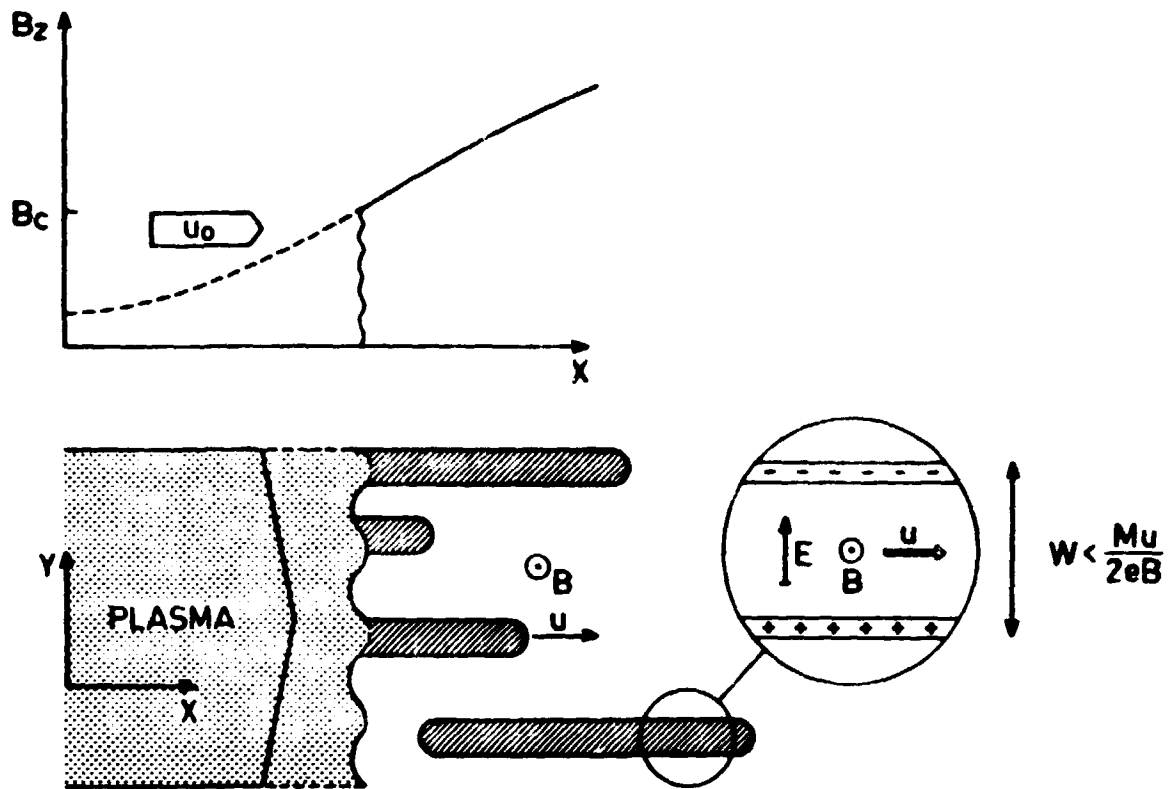


Figure 1 A schematic picture of a plasma beam penetration into perpendicular magnetic field. The width of  $E \times B$  penetrating structures is constrained by the half of an ion gyroradius  $w < \frac{Mu}{2eB}$ .

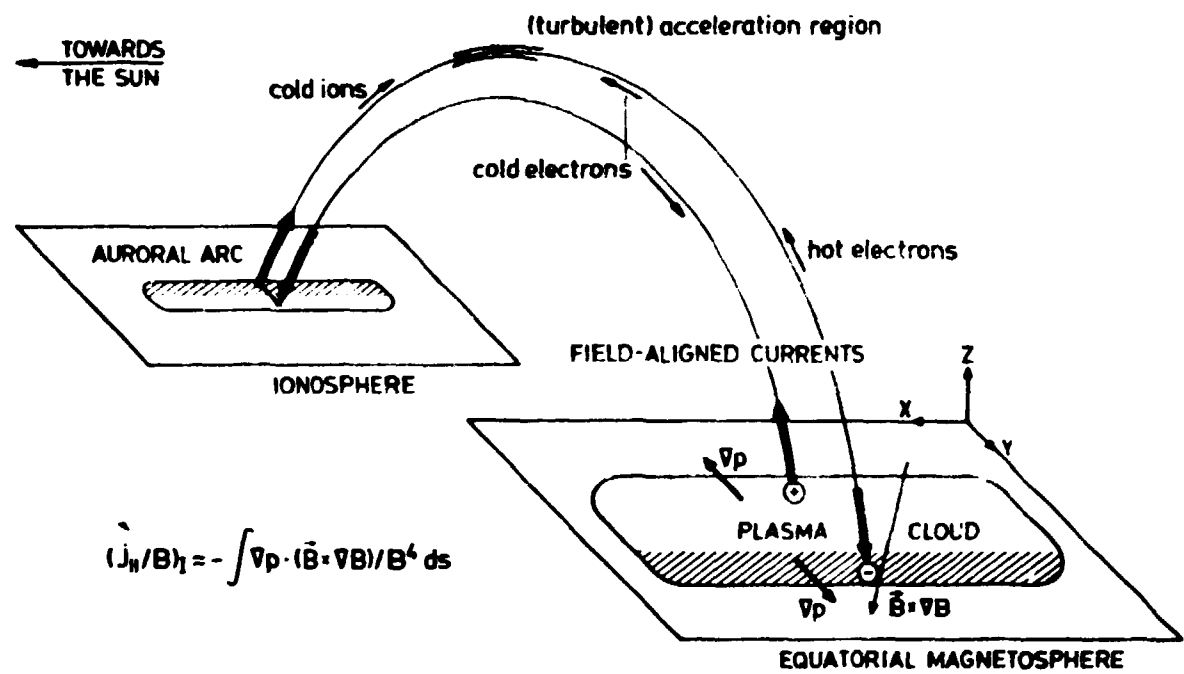


Figure 2 Establishment of field-aligned currents driving an auroral arc due to the presence of a low-pressure plasma cloud in the equatorial magnetosphere. Symmetrical currents into the conjugate ionosphere are not shown.